Aquat Sci (2014) 76 (Suppl 1):S33–S46
DOI 10.1007/s00027-013-0313-8

Aquatic Sciences

RESEARCH ARTICLE - BASED ON MIR INVESTIGATIONS IN LAKE GENEVA

Bacterial communities in trace metal contaminated lake sediments are dominated by endospore-forming bacteria

Loïc Sauvain · Matthieu Bueche · Thomas Junier · Matthieu Masson · Tina Wunderlin · Roxane Kohler-Milleret · Elena Gascon Diez · Jean-Luc Loizeau · Mary-Lou Tercier-Waeber · Pilar Junier

Received: 21 December 2012 / Accepted: 14 September 2013 / Published online: 26 October 2013

Abstract Lake sediments in areas close to the outlet of wastewater treatment plants are sinks for pollutants. Bacterial communities in sediments are likely affected by the released effluents, but in turn they might modify the distribution and bioavailability of pollutants. On the shore of Lake Geneva, Switzerland, wastewater from the City of Lausanne is treated and discharged into the lake via an outlet pipe in the Vidy Bay. The objectives of this study were to assess (1) the impact of the treated wastewater release on the bacterial communities in the Vidy Bay sediments and (2) the potential link between bacterial communities and trace metal sediment content. Bacterial community composition and abundance were assessed in sediments collected in three areas with different levels of contamination. The main factors affecting bacterial communities were inferred by linking biological data with chemical analyses on these sediments. Near to the outlet pipe, large quantities of bacterial cells were detected in the three upper most cm (3.2×10^9 cells assessed by microscopy and 1.7×10^{10} copies of the 16S rRNA gene assessed by quantitative PCR, per gram of wet sediment), and the dominant bacterial groups were those typically found in activated sludge (e.g. *Acidovorax defluivii* and *Hydrogenophaga caeni*). Three samples in an area further away from the outlet and one sample close to it were characterized by 50 % of endospore-forming Firmicutes (*Clostridium* spp.) and a clear enrichment in trace metal content. These results highlight the potential role of endospore-forming Firmicutes on transport and deposition of trace metals in sediments.

Keywords Sediments · Bacterial communities · Firmicutes · Trace metals · High-throughput DNA sequencing · Lake Geneva

This article is part of the special issue "éLEMO – investigations using MIR submersibles in Lake Geneva".

Electronic supplementary material The online version of this article (doi:10.1007/s00027-013-0313-8) contains supplementary material, which is available to authorized users.

L. Sauvain · M. Bueche · T. Junier · T. Wunderlin · P. Junier (✉)
Laboratory of Microbiology, University of Neuchâtel, Rue Emile Argand 11, 2000 Neuchâtel, Switzerland
e-mail: pilar.junier@unine.ch

M. Masson · M.-L. Tercier-Waeber
Analytical and Environmental Chemistry, Department of Inorganic and Analytical Chemistry, University of Geneva, Geneva, Switzerland

R. Kohler-Milleret
Laboratory Soil and Vegetation, University of Neuchâtel, Neuchâtel, Switzerland

E. Gascon Diez · J.-L. Loizeau
Earth and Environmental Science Section, Institute F.-A. Forel, University of Geneva, Geneva, Switzerland

Introduction

Access to clean drinking water is undoubtedly one of the major concerns for humans. However, agricultural, industrial, and domestic activities lead to increasing chemical contamination of freshwater via runoff or wastewater discharge (Schwarzenbach et al. 2006; Förstner and Wittmann 1981). In industrialized countries, wastewater treatment plants (WWTPs) remove a large fraction of contaminants. Nevertheless a significant quantity of chemicals are still not efficiently retained or broken down during the process and their release into aquatic environments remain a significant

concern for environmental and public health (Schwarzenbach et al. 2006). Therefore, we still need to understand how to deal not only with the sources, but also with the fate of these contaminants that may accumulate over-time. Among the inherently persistent contaminants are the trace metals (TMs), which are involved in biogeochemical cycles in aquatic ecosystems and distributed in various chemical forms, including inorganic and organic colloids as well as particulate matter (Tercier-Waeber et al. 2012). Colloids and particulate matter (through coagulation, aggregation and sedimentation) play a key role in the transport of TMs from the water column to the sediment. Thus, sediment is one of the major sinks of TM contaminants (Schwarzenbach et al. 2006; Poté et al. 2008; Thevenon et al. 2011a).

Bacteria, through their diverse metabolic activities and large combined biomass, play a key role in biochemical cycles in aquatic sediments (Nealson 1997). In particular, bacterial metabolic activity can facilitate the remobilization of TMs from the sediment into the water column (Förstner and Wittmann 1981; Zhang et al. 1996). An example of this is the methylation of mercury occurring in anaerobic sediments, which is accelerated by in situ sulfate- and iron-reducing bacteria (such as *Geobacter* sp.) (Kerin et al. 2006; Benoit et al. 2003; Yu et al. 2012). Methyl-mercury is a neurotoxin that is transferred through the food chain by bioaccumulation, representing a major risk of intoxication in humans via consumption of contaminated fish (Selin 2009). Hence, remobilization of TMs adsorbed in the sediment increases their potential (eco)toxicity impact, creating a threat to the aquatic ecosystem, as well as human health (Förstner and Wittmann 1981; Schwarzenbach et al. 2006). Therefore, it is essential to improve our knowledge of the effect of TMs on microbial communities in contaminated sediments, as well as the effect of microbial activities on TM immobilization and remobilization.

Various approaches have been taken to study the link between microbial communities and metal pollution in sediments. One approach is the concept of pollution-induced community tolerance (PICT), developed as a sensitive tool to detect minor effects of anthropogenic pollution on biological communities (Blanck et al. 1988; Blanck 2002). A recent study shows that PICT could be evaluated to test the effect of chronic metal pollution on estuarine sediment microbial communities (Ogilvie and Grant 2008). A link between pore water copper concentrations and PICT was observed. However, no correlation between community structure and development of tolerance to metals was found. Another study investigating the community structure in anoxic freshwater sediments along a gradient of contamination with zinc also failed to find a correlation between community structure and various levels of zinc and arsenic (Gough and Stahl 2011). One of the reasons for this is that a broad approach consisting in the evaluation of the whole microbial community may miss more subtle changes in specific functional groups. For example, a study investigating the effect of mercury associated to tailings from the Idrija Mine showed the presence of mercury detoxification genes solely downstream from the discharge into the river with the same name, compared to upstream (Hines et al. 2000). In other naturally enriched environments such as the Rio Tinto in Spain, sulfate-reducing bacteria have been shown to be associated with the attenuation of the effect of acid mine drainage (AMD) thanks to the immobilization of metals in insoluble sulfides (Sánchez-Andrea et al. 2012). In other cases, sulfate-reducers have been associated with the production of methyl-mercury in AMD impacted sediments (Batten and Scow 2003; Shipp and Zierenberg 2008). Those examples are not exclusive of aquatic ecosystems as similar targeted effects have been observed in Cu-contaminated soils (Berg et al. 2012).

Another microbial group that can be of particular interest is the group of endospore-forming bacteria (EFB), belonging to the phylum Firmicutes. Endospores are highly specialized structures that allow bacteria to remain dormant for long periods of time under unfavorable environmental conditions (Errington 2003) and could be an efficient strategy to survive in polluted environments. Recent reports support this hypothesis, especially with respect to trace metals. Field studies of microbial communities present in U-contaminated sites (Anderson et al. 2003; Chang et al. 2001), as well as in drainage water contaminated with Pb, Cu and Zn (Nakagawa et al. 2002) suggested that EFB are important and might tolerate pollution better than non-spore formers. However, in the case of more common and widely spread anthropogenic sources of pollution, such as effluents of urban or industrial wastewater treatment plants, there is a gap of knowledge on the prevalence and diversity of EFB.

The aim of this project is evaluating the abundance and diversity of bacterial communities in lake sediments and the potential influence of TM contamination on these parameters. To achieve this, sediment samples were collected in three areas differentially impacted by the WWTP effluent of the City of Lausanne according to previous studies (Thevenon et al. 2011a, b; Poté et al. 2008; Wildi et al. 2004; Pardos et al. 2004; Loizeau et al. 2004; Bravo et al. 2011). Bacterial abundance and diversity were assessed using the 16S rRNA gene as a universal bacterial molecular marker. High-throughput DNA sequencing was conducted to obtain an overview of the bacterial community composition. This type of analysis allows the recovery not only of the dominant groups, but also rare members of the community. In the sequence analyses, particular

emphasis was placed on assessing the prevalence of EFB. Finally, a characterization of the sediments was conducted to infer the influence of chemical factors on the changes in the microbial community composition.

Materials and methods

Study site

Lake Geneva (580 km^2, 89 km^3, maximum depth 310 m), nowadays considered mesotrophic (Dorioz et al. 1998), is one of the largest freshwater reservoirs of Europe and currently provides drinking water for approximately 700,000 inhabitants (Poté et al. 2008). In the WWTP of Lausanne, Switzerland, serving one of the largest cities along the shore of Lake Geneva (236,000 population equivalents), 92,400 m^3/day of water were released into the lake, from which 9,900 m^3/day were untreated (release from combined sewage overflow; SESA 2012). The outlet of the WWTP is located within the Vidy Bay at 700 m from the lakeshore at a depth of 35 m. A previous study showed that the highest TMs levels in the sediment of the Vidy Bay were found around the outlet of the WWTP as shown in Fig. 1a (Poté et al. 2008). Total mercury concentrations of up to 8.7 mg/kg (dry weight sediment) were measured in this area (Poté et al. 2008), and it has been reported that methyl-mercury follows a similar trend (Bravo et al. 2011). Mercury values are about 18 times higher than the probable effect levels (PELs) indicated by the Canadian Sediment Quality Guidelines (CCME 1999); and more than four times higher than the limit concentration for relevant sediment contamination, accordingly to the International Commission for the Protection of the Rhine (ICPR) (ICPR 2009).

Sampling

In order to obtain a large variation in particulate TM concentrations, sampling sites were determined on the basis of measurements published previously (Poté et al. 2008) (Fig. 1a). Six cores were collected during two sampling campaigns. Two initial cores were collected with the MIR submersible during the sampling campaign of the ELEMO project (July 2011), in a supposedly moderately contaminated area (about 300–400 m from the outlet pipe), which were coded with the letter M (M1 and M2). Four additional cores were retrieved in October 2011 from a boat; two of the cores near the outlet pipe of the WWTP (i.e. supposed as the highest contaminated area), hereafter indicated by the letter N (N1 and N2); and two from an area with supposedly low particulate TM, distal to the outlet pipe (indicated by the letter D as D1 and D2). During both campaigns Plexiglas tubes of 6 cm (diameter) were used as push-cores for the sediments. At the laboratory, the cores were sub-sampled under sterile conditions. If immediate sub sampling was not possible, the cores were stored at 4 °C and the overlaying water was bubbled with air in order to preserve the oxygen gradient at the sediment–water interface. Two top layers were analyzed separately in triplicates: 0–3 cm, indicated as upper; and 3-9 cm, indicated as lower.

Chemical analysis

Water content of the sediment was estimated weighting the sediment before and after freeze-drying. Another fraction of the sample was used for chemical analysis. Prior to the analysis of chemical compounds adsorbed onto the sediments, they were air-dried and agate ground. Total particulate organic carbon ($C_{org\text{-}part}$) and nitrogen (N_{part}) were measured with a CHN-analyzer (CHNEA1108-Elemental analyser, CE Instruments Ltd, Wigan, UK) following a carbonate fumigation exposing the samples to concentrated HCl vapors for 6 h (Harris et al. 2001). After Kjeldahl oxidation, total phosphorus was determined colorimetrically at 880 nm using the molybdate procedure (Murphy and Riley 1962). X-ray fluorescence (XRF) was performed with the Uniquant® method (Thermo Fisher Scientific, Vantaa, Finland) to quantify sulfur. Total particulate TM concentrations were measured by quadrupole-based Inductively Coupled Plasma-Mass Spectrometry (ICP-MS) (HP 4500, Agilent Technologies, Santa Clara, CA, USA) following an aqua regia digestion (Förstner and Wittmann 1981). The standard "LKSD-4" was used as control to validate the metal quantification. Additional measurements of particulate metal concentration were obtained by XRF. These values were used for the extrapolation of particulate metal concentration shown in Fig. 1b, c. Finally, total mercury was quantified by atomic absorption spectrometry (AAS) (Advanced Mercury Analyser; AMA 254, Altec, Dvůr Králové nad Labem, Czech Rep.).

Extraction of cells from sediments

Three grams of wet sediment were mixed with a dispersing solution (1 % Na-hexametaphosphate) in a ratio of 1/5 and homogenized 2 × 1 min at 15,500 rpm using an Ultra-Turrax® homogenizer (T18 basic ULTRA-TURRAX®, IKA, Staufen, Germany). The heaviest mineral particles were removed by sedimentation (10 min) allowing the recovery of the cells contained in the supernatant. The extraction was repeated once more with an equal volume of the dispersion solution. The two supernatants were pooled together and centrifuged at low speed (20 g for 1 min) in

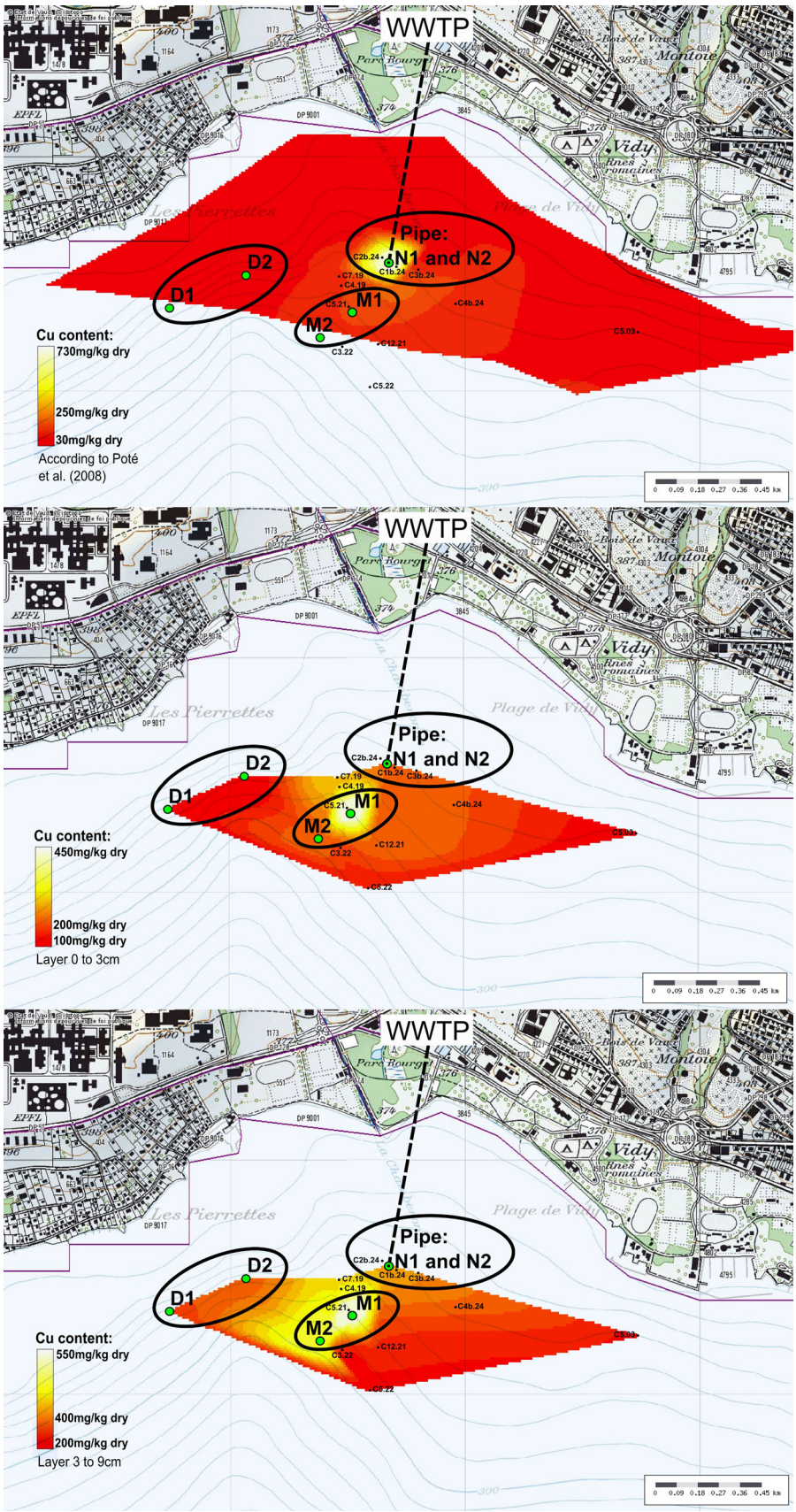

Fig. 1 Map of the Vidy Bay indicating the positions of the cores retrieved with the MIR submersible or with the boat from the F-A Forel Institute (*green dots*). The pipe (*dashed line*) rejecting the wastewater treated by the WWTP from Lausanne is also shown. The cores were retrieved near (N1 and N2) the pipe, or at middle (M1 and M2) and distal (D1 and D2) positions from it. For this study three areas were selected based on previously reported Hg concentrations (Poté et al. 2008) as shown in **a**, and are indicated by *black circles*. Two cores per area were considered for the analyses. Current Cu concentrations measured by XRF in the upper layers (**b**) and lower layer (**c**) are presented for comparison with the previously published Hg values (color figure online)

order to remove the remaining sediment particles and to recover a final supernatant containing cells and spores. From this final supernatant, 30 µL were kept to perform fluorescence microscopy, while the rest (about 24 mL) was divided into two equal fractions, and each one was filtered onto two different 0.2 µm pore-size nitrocellulose filters (11407-47-CAN, Sartorius, Goettingen, Germany) and stored at −80 °C. One of the filters was kept as a back-up.

Fluorescence microscopy (FM) and cell counting

The 30 µL of sediment extract (recovered cells from the sediment) were diluted 50× in a saline solution (0.015 % NaCl) containing 2 % formalin for fixation. Then 500 µL of the diluted cell extract were filtered through black 0.2 µm pore-size nitrocellulose filters (GTBP02500, Millipore, Billerica, MA, USA). Filters were placed on microscopy slides with 50 % glycerol and 50 % Tris–EDTA and stained for 15 min with a SYBR® Green I 20× solution (adapted from (Weinbauer et al. 1998). The stained filters were observed at a magnification of 1,000× with an epifluorescence microscope using filter cube L5 (Leica DMR, Leica Microsystems, Wetzlar, Germany). Ten random images were taken per filter and automatic counting of the cells was performed using the program *daime* (Daims et al. 2006).

DNA extraction and precipitation

DNA was extracted using the MP FastDNA® SPIN Kit for Soil (MP Biomedicals, Santa Ana, CA, USA). This kit has been chosen because of its ability to extract DNA from endospores compared to other kits (Dineen et al. 2010). A modified protocol was applied in order to better extract DNA from hard-to-lyse cells and endospores. Briefly, the modified protocol consisted of three consecutive bead-beating steps treated separately following the manufacturer instruction before being pooled together at the end of the procedure. Total DNA was then precipitated from the aqueous phase by adding sodium acetate [final concentration of 0.3 M (pH 7.6)] and 2 volumes of ice-cold pure ethanol. DNA was incubated in ice for 1 h and collected by centrifugation (1 h at 21,460×g and 4 °C). The supernatant was removed and the precipitate washed with 1 mL of cold 70 % ethanol and centrifuged again (30 min at 21,460×g and 4 °C). A maximum of supernatant was removed and the remaining droplets were evaporated by vacuum centrifugation (Univapo 150H, Uniequip, Planegg, Germany) for 5 min. DNA was resuspended in 50 µL of PCR-grade water. Total DNA was quantified before and after ethanol precipitation with Qubit® 2.0 Fluorometer (Invitrogen, Carlsbad, CA, USA) to calculate the recovery rate of DNA.

Real-time PCR on the 16S rRNA gene

Real-time PCR on the V3 region of the 16S rRNA gene was performed with a Corbett Rotor-Gene 3000 (Qiagen, Hilden, Germany) using the primers 338f (5′-ACTCCTACGGGAGGCAGCAG-3′) and 520r (5′-ATTACCGCGGCTGCTGG-3′) (Bakke et al. 2011; Muyzer et al. 1993), which are routinely used to asses bacterial abundance or to carry out profiling of bacterial communities. Reaction mix consisted of DNA template (ranging between 0.5 and 20 ng), 0.3 µM of each primer and 1× Rotor-Gene SYBR Green PCR Master Mix (Qiagen). Total reaction volume of 10 µL was reached with PCR-grade water. The program started with a hold at 95 °C for 15 min to activate the polymerase (HotStarTaq *Plus* DNA Polymerase) followed by 40 cycles of denaturation at 95 °C for 10 s, annealing at 55 °C for 15 s and elongation at 72 °C for 20 s. The number of gene copies was calculated by comparison with a standard curve using dilutions from 10^8 to 10^2 copies/µL of a plasmid containing the V3 sequence from an environmental clone prepared with the Invitrogen™ Zero Blunt® TOPO® PCR Cloning kit for sequencing and inserted in competent *E. coli* cells (Invitrogen™ One Shot® TOP10). Plasmid extraction was performed with the Wizard® Plus SV Miniprep DNA Purification System (Promega, Madison, WI, USA) following manufacturer instructions. The DNA concentration was deduced from the quantification with Qubit® 2.0 Fluorometer (Invitrogen) of the final plasmid product.

PCR amplification of the 16S rRNA gene and denaturing gradient gel electrophoresis (DGGE)

The V3 variable region of the 16S rRNA gene was amplified using the primers GC 338f (5′-GC-clamp-ACTCCTACGGGAGGCAGCAG-3') and 520r (Bakke et al. 2011; Muyzer et al. 1993). PCR reactions were performed in a total volume of 50 µL containing: 1 ng of DNA template, 1× ThermoPol Reaction Buffer (New England Biolabs, Ipswich, MA, USA), 1.25 U of Taq DNA Polymerase (New England Biolabs), 3 mM of $MgCl_2$, 0.25 µM of each primer (Microsynth, Balgach, Switzerland) and 0.2 µM of each dNTP (Promega). PCR amplifications were carried out with a Thermo Scientific Arktik Thermal Cycler (Thermo Fisher Scientific). PCR program consisted of an initial denaturation at 94 °C for 10 min, followed by 10 cycles with denaturation at 94 °C for 30 s, annealing at 65 °C (touchdown of −1 °C/cycle) for 30 s and elongation at 68 °C for 30 s, the following 25 cycles consisted of denaturation at 94 °C for 30 s, annealing at 55 °C for 30 s and elongation at 68 °C for 30 s. The amplification was completed by a final elongation at 68 °C for 5 min. PCR products were verified by standard 1.2 % agarose gel

electrophoresis. To obtain enough DNA to conduct the DGGE analysis (minimum 600 ng), two PCR products of each sample were pooled together and concentrated by vacuum centrifugation (Univapo 150H, Uniequip) during 45 min.

DGGE was carried out in a Bio-Rad D-Code Universal Detection Mutation system (Bio-Rad Laboratories, Hercules, CA, USA). 8 % acrylamide gels with a 30–60 % gradient of denaturants (with 100 % of denaturants consisting of 40 % (vol/vol) formamide and 7 M urea) (Muyzer et al. 1993) were cast between two glass plates (16 by 16 cm), 1.5 mm spacers and 1 cm-wide loading wells. A minimum of 600 ng of DNA in 20 µL was mixed with 5 µL of loading buffer (60 % sucrose, 0.25 % bromophenol blue and 0.25 % xylencyanol FF) and loaded into the wells (Ferris et al. 1996). Runs were conducted at 60 °C with a constant voltage of 150 V during 4 h 30 min in 1× TAE buffer (0.04 M Tris base, 0.02 M sodium acetate and 1 mM EDTA; pH adjusted to 7.4). Then the gels were stained with 1X SYBR® Gold (Invitrogen) during 30 min and visualized using the GenoPlex system (VWR, Radnor, PA, USA). GelCompar II (Applied Maths, Sint-Martens-Latem, Belgium) and the open source R software, (www.r-project.org/) was used for statistical analysis of the gels. To allow the comparison of different gel images, a ladder containing PCR products from ten strains (50 ng per strain) having different G-C contents and resulting in a pattern of bands distributed throughout the gel, was loaded on each side of the gel.

Pyrosequencing and bioinformatic analysis

High-throughput DNA amplicon sequencing on the V1-V3 variable regions of the 16S rRNA gene was conducted by Eurofins MWG Operon (Ebersberg, Germany) using GS FLX+ technology (454 Life Sciences, Branford, CT, USA). The primers Eub8f (5′-AGAGTTTGATCCTGG CTCAG-3′) and Eub519r (5′-GTATTACCGCGGCTGCT GG-3′) were used. These primers were selected based on recent results indicating that this region is the best performing for profiling and identification of diverse members of bacterial communities (Li et al. 2009). The sequences (about 20,000 per sample) sent by Eurofins MWG Operon, were compared by BLASTN (Altschul et al. 1990) (http://www.ncbi.nih.gov) to a 16S rRNA gene database of 8911 sequences (the most complete database available, containing only good quality sequences of type strains downloaded from the Ribosomal database project; http://rdp.cme.msu.edu/), and containing well-described groups of iron- and sulfate-reducing bacteria that could be expected in metal-contaminated sediments. For each analyzed sequence only the closest hit in the reference database was conserved. In addition the sequences were clustered into putative OTUs (identity of >95 %) and identified with the pick_otus_through_otu_table.py script from the QIIME package (Caporaso et al. 2010).

Statistical analysis

A first set of multivariate exploratory analyses was conducted with the R software and the package *vegan*. Pearson correlations were calculated between chemical elements and/or between bacterial abundance measured by FM and real-time quantitative PCR. Canonical correspondence analysis (CCA) was selected to analyze the relationship between the environmental factors and the composition of the bacterial communities. In this analysis the bacterial groups that constitute the communities of the different samples were constrained with the data of environmental variables. This analysis was selected because it allows establishing a correspondence between changes in abundance and variation of environmental conditions, and takes into consideration rare species, which are obtained during high-throughput DNA sequencing (Ramette 2007). The CCA was carried out following the procedure described in the vegan tutorial. Diversity indexes (Shannon and Evenness) were calculated using R. Finally the chao1 index was used as a statistical estimator of species richness in a rarefaction analysis (Colwell and Coddington 1994). Rarefaction curves (Chao1) were calculated using the script alpha_rarefaction.py in QIIME.

Results

Chemical analysis

Analyses of the 12 samples (six cores and two depths) showed a large variation of the sediment chemical composition (Table 1). For half of the cores (N1, D1, and D2), the upper sediment layer (0–3 cm) contained higher $C_{org\text{-}part}$ than the lower layer (3–9 cm). The highest $C_{org\text{-}part}$ contents were measured in core M1 (both layers), respectively with 7 and 7.72 % (of total dry sediment weight). The lowest $C_{org\text{-}part}$ levels were found in the sediments sampled further away from the outlet pipe (D1 and D2). A similar trend for the N_{part} content was found but with a range varying between 0.17 and 0.65 %. Total particulate phosphorous ranged from 0.08 to 0.38 %, measured in the upper layer of core D1 and the upper layer of core N1, respectively. The highest particulate concentration of sulfur was measured in the upper layer of core N2, with 1.4 % while the lowest concentration was measured in the upper layer of core D2 with 0.43 %. The water content of the sediments varied from 57 to 72 % (Table 1). Particulate manganese showed small variability with values ranging

Table 1 Location of the sampling sites and chemical data of six sediment cores collected near the outlet pipe of the WWTP of Lausanne, in the Vidy Bay, Switzerland

Expected level of HM (according to Poté et al. 2008)	Core	Sampling site locations (Swiss coordinates)		Layer[a] (cm)	ω (%)	C_{org} (%)	N (%)	P (%)	S (%)	Mn (mg/kg)	Fe (g/kg)	Hg (mg/kg)	Cu (mg/kg)	Zn (mg/kg)	Cd (mg/kg)	Pb (mg/kg)	As[b] (mg/kg)	Al[b] (g/kg)
		X (m)	Y (m)															
Low	D1	533,735	151,351	0–3	69.61	2.67	0.23	0.08	0.48	408	18.2	0.24	75	170	0.74	43	8	16.3
				3–9	62.98	2.64	0.21	0.11	0.76	387	19.9	0.84	114	322	1.90	124	10	13.9
	D2	534,063	151,491	0–3	69.64	2.78	0.23	0.10	0.43	405	24.8	0.27	81	205	0.81	53	9	15.3
				3–9	57.14	2.36	0.17	0.29	0.94	396	22.5	0.80	137	542	2.76	154	9	9.2
Medium	M1	534,515	151,335	0–3	71.67	7.00	0.53	0.24	1.19	390	43.5	*7.65*	*292*	*1,032*	*6.27*	*311*	*15*	*18.6*
				3–9	73.10	7.72	0.65	0.17	0.98	413	47.8	*8.98*	*362*	*1,564*	*10.13*	*498*	*22*	*20.8*
	M2	534,379	151,229	0–3	71.75	4.01	0.38	0.14	0.69	415	33.2	0.87	165	399	1.66	100	13	17.7
				3–9	64.84	5.08	0.40	0.34	0.86	400	34.3	*1.25*	*293*	*974*	*4.38*	*274*	*16*	*16.3*
High	N1	534,676	151,543	0–3	79.27	5.96	0.62	0.38	ND[c]	392	40.0	1.42	155	416	1.88	115	13	13.4
				3–9	66.32	3.79	0.31	0.23	1.20	443	33.9	1.15	123	349	1.76	97	11	16.2
	N2	534,676	151,543	0–3	75.38	4.69	0.46	0.32	1.40	369	35.8	1.30	129	346	1.59	127	11	13.0
				3–9	71.35	6.30	0.58	0.20	1.19	401	36.0	*2.85*	*341*	*902*	*8.06*	*294*	*22*	*21.4*

In each core two independent depths (upper 0–3 cm; lower 3–9 cm, column layer) were analyzed. ω water content. All values measured in dry sediments. Metal content measured in mg/kg, except for Fe and Al. *ND* not determined. Samples containing elevated heavy and trace metal concentrations (Hg, Cu, Zn, Cd, Pb, As, and Al) are indicated in italic

[a] Layer analyzed (in centimeter from the top of the core)

[b] Values of As and Al only considered as indicatives (quantification not accurate)

[c] Not determined due to a lack of sediment remaining for the analysis

from 369 to 443 mg/kg. The maximum particulate iron content was found in the lower layer of core M1 and the minimum in the upper layer of core D1, with 4.8 and 1.8 g/kg, respectively.

A general overview of TM_{part} concentration obtained by XRF on 11 cores (including the 6 cores of the present study) showed that for the upper layer, the highest values are not found in the vicinity of the outlet pipe (comparison between Fig 1a, b). For the lower layer, the TM_{part} contaminated area is more diffuse and included sediment cores in close vicinity to the outlet pipe (N2) as well as those retrieved in the area supposedly containing intermediate TM_{part} concentrations (M1 and M2). Accordingly, samples that contained elevated TM_{part} concentrations measured by ICP-MS corresponded to those areas identified by XRF. Four samples contained relatively elevated TMs concentrations (Table 1): the lower layer of the cores N2 and M2 and both layers of the core M1. The highest levels of each TM_{part} were found in the lower layer of core M1, with 8.98 mg/kg of Hg, 362 mg/kg of Cu, 1,564 mg/kg of Zn, 10.13 mg/kg of Cd, and 498 mg/kg of Pb. The lowest TM_{part} contents were measured in the upper layer of the cores D1 and D2, both sampled in the distal area, supposedly less influenced by the outlet pipe of the WWTP. Measurements of particulate As and Al were only considered as indicative because the measurement of the standard LKSD-4 was not accurate for these two elements. Pearson correlation matrix (Supplementary Fig. 1) revealed significant positive correlations between $C_{org\text{-}part}$, N_{part}, Fe_{part} and all TM_{part} concentrations. The S_{part} concentration was also positively correlated with P_{part} and Fe_{part} content.

Table 2 Bacterial abundance and diversity in sediment cores of the Vidy Bay

Core	Layer (cm)	Fluorescence microscopy (cells/g)[a]	Real-time PCR (copies of gene/g)[a]	Shannon index (H′)	Evenness (J)
D1	0–3	1.3×10^9	3.3×10^9	5.62	0.77
	3–9	2.2×10^9	4.3×10^8	5.36	0.74
D2	0–3	1.2×10^9	1.5×10^9	5.48	0.76
	3–9	1.3×10^9	6.2×10^7	5.31	0.74
M1	0–3	6.9×10^8	3.2×10^8	4.57	0.64
	3–9	8.0×10^8	5.3×10^8	4.25	0.61
M2	0–3	5.1×10^8	1.7×10^9	5.1	0.72
	3–9	7.1×10^8	2.8×10^8	4.25	0.61
N1	0–3	2.6×10^9	1.7×10^{10}	4.69	0.66
	3–9	1.1×10^9	6.1×10^8	5.45	0.77
N2	0–3	3.2×10^9	1.2×10^{10}	5.08	0.71
	3–9	1.5×10^9	4.7×10^8	4.39	0.61

Shannon index and evenness were strongly correlated ($R^2 > 0.98$)

[a] Cells and copies of gene measured per gram of wet sediment

Quantification of bacterial communities

Quantification of bacterial abundance resulted on average in 1.4×10^9 cells (fluorescent microscopy, FM-) and 3.2×10^9 16S rRNA gene copies (real-time quantitative PCR) per gram of wet sediment. This represented a mean of 2.3 copies of 16S rRNA gene per cell. Both analyses revealed the largest abundance of bacteria in the upper layer of cores N1 and N2 sampled near the outlet pipe of the WWTP, with 2.6 and 3.2×10^9 cells/g counted by FM, and 1.7×10^{10} and 1.2×10^9 copies of gene/g measured by real-time PCR, respectively (Table 2). The lowest abundance of cells was found in both layers of cores M1 and M2, whereas the lowest gene copy numbers were measured in the lower layer of core D2. A significant correlation (p value of 0.05; Supplementary Fig. 1) was found between the two methods used to measure bacterial abundance.

Bacterial community fingerprinting

Fingerprinting analysis by DGGE showed high reproducibility between triplicates of each sample (data not shown). Thus, in order to compare the bacterial community composition between the 12 samples, a gel containing the three replicates pooled together was generated (Fig. 2). This allowed an improved analysis by avoiding differences between gels (e.g. migration or staining). All profiles showed a large number of bands (more than 70 bands per lane), attesting an important bacterial diversity in both layers and in each core. Fingerprints clearly differed between the cores corresponding to the three areas of sampling and between the two layers of a same core. A similar band pattern was observed in cores D1 and D2 (both layers), upper layer of cores N1 and N2, and lower layer of cores M1 and M2. In contrast, this was not the case for fingerprints corresponding to the upper layer of cores from the intermediary area (M1 and M2) and to the lower layer of cores sampled near the outlet pipe (N1 and N2). A pattern of two strong bands located in the region of high denaturant concentration (black squares in Fig. 2; lane 4 of layer 0–3 cm and lanes 3, 4 and 6 of layer 3–9 cm) was detected in the four samples of highest TM_{part} levels (M1upper, M1lower, M2lower and N2lower).

Pyrosequencing and bioinformatics analyses

Close to 22,000 sequences per sample were obtained by pyrosequencing. The sequences matched 3,388 different type strains (out of 8,911) from the reference database in a BLAST search (data not shown). The eight most abundant species identified in each sample are presented in Supplementary Fig. 2. Sequences were assigned to an OTU at the

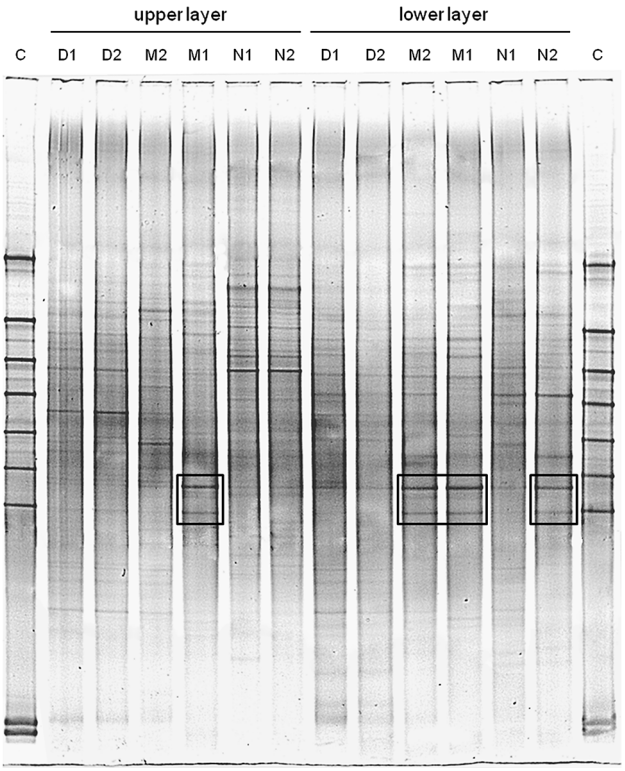

Fig. 2 DGGE profiles for the V_3 region of the 16S rRNA gene of the bacterial communities in sediment cores collected in the Vidy Bay. For labeling of the samples see Fig. 1. The two *lanes* C correspond to the ladder. A pattern composed by two strong bands located in the region with high denaturant concentration was found in the lanes corresponding to sediments with high particulate trace metal content (Table 1) and is indicated by *black squares*

species level with >97 % identity, at the genus level with >95 % identity and at the phylum level with >80 % identity (Schloss and Handelsman 2005; Stackebrandt and Goebel 1994). In the four samples containing the highest TM_{part} levels (M1upper, M1lower, M2lower and N2lower) the most abundant OTU found was identified at the species level as the endospore-forming bacterium *Clostridium lituseburense*, which represented 19–21 % of the total of sequences. Two other endospore-forming bacteria, *Clostridium bartletti* and *Clostridium disporicum,* corresponded to the second or third most abundant species detected in TM-contaminated sediments. All together *Clostridium* spp. represented up to 49 % of the total sequences in the four samples with high TM_{part} content, but reached a maximum of 10 % in the other sediments. *C. lituseburense* was also found among the eight most abundant species identified (except for D1upper and D2upper) in other samples, but represented about 4 % of the community.

In the upper layer of the two cores sampled near the outlet pipe, the dominant species was *Hydrogenophaga caeni* (identified at the species level), representing 22 % and 14 % of the sequences in samples N1upper and

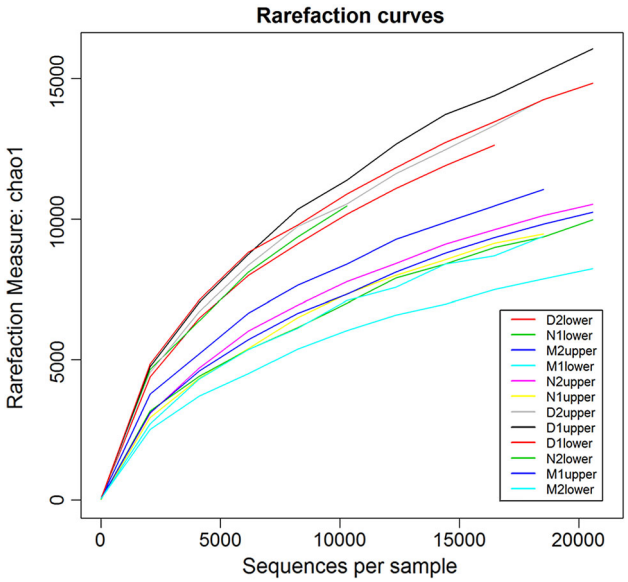

Fig. 3 Rarefaction curves for the 12 samples showing the diversity detected compared with the predicted total diversity. The x axis represents the number of sequences sampled while the y axis represents a measures of the species richness detected, estimated with the Chao1 index. The *legend* on the *bottom right* shows the correspondence between the curves and the samples. For labeling of the samples see Fig. 1

N2upper, respectively. In the same samples the second most abundant species assigned (6 and 7 % of the total sequences) was *Acidovorax defluvii*. In sample N1lower the two most abundant assigned OTUs (over 5 % of the sequences) were related to the phylum Chloroflexi and *C. lituseburense*. For both layers of core D1 and in the upper layer of core D2 retrieved from the distal area, the majority of the sequences were affiliated to the (per)chlorate-reducing bacteria related to *Dechloromonas* spp. The highest proportion of the sequences (6 %) from lower layer of the sample D2 was most closely related to the Gammaproteobacteria. In the upper layer of the core M2, which did not show a high TM_{part} concentration (Table 1), the two most abundant assigned OTUs were the Fe(III)-reducing *Geobacter* spp. (Nevin et al. 2005) and *D. hortensis*, with 9 and 6 % of total sequences, respectively.

Based on the pyrosequencing data, the Shannon index (H′) and evenness (J) (Table 2) were calculated to obtain a global overview of the diversity of bacterial communities in the sediment samples. The highest diversity was found in the upper layer of cores D1 and D2, and in the lower layer in core N1. The lowest values were found in the lower layer of the cores M1, M2 and N2, i.e. sediment core layers characterized by the highest TM_{part} concentrations (Table 1). The logarithmic shapes of the rarefaction curves obtained for the sequence data (Fig. 3) indicated that most of the species richness occurring in the sediments was detected. Indeed as the identification of sequences progressed (x axis), the detection rate for new species leveled off (y axis).

Canonical correspondence analysis (CCA)

An ordination plot of the samples was constructed using the results of pyrosequencing after OTU picking and identification of species using QIIME (Fig. 4). Three principal groups of samples were observed. The groups corresponded to the clustering based on the DGGE analysis (data not shown). Based on the community composition the four samples with high TM_{part} levels (M1upper, M1lower, M2lower and N2lower) formed a group in the bottom right part of the plot. Accordingly, the vectors Cd, Pb, Cu, Hg, and As are the environmental factors that corresponded more significantly the community composition in this group of samples. This group is also characterized by the prevalence of endospores-forming bacteria. As previously outlined (Supplementary Fig. 2) the prevalence of endospore-forming bacteria belonging to the Firmicutes (mainly Clostridiaceae, *Clostridium* spp., *Sarcina* spp., *Syntrophomonas* spp.) in these samples is clearly highlighted in the CCA.

The samples from the upper layer of the cores N1 and N2, near the outlet pipe of the WWTP, formed a second group (in the top right part of the plot). The community composition was characterized by non-endospore-forming Firmicutes (e.g. *Streptococcus* spp.) and non-Firmicutes (e.g. *Acidovorax* spp. and Comamonadaceae, corresponding to the identification of *H. caeni* by BLAST in Supplementary Fig. 2. However, endospore-forming bacteria were not enriched in these samples.

The remaining samples (D1upper, D1lower, D2upper, D2lower, M2upper and N1lower) represented a third group anti-correlated with all environmental factors, except Mn, but correlated with a large diversity of bacteria phyla such as Betaproteobacteria (*Dechloromonas* spp, *Thiobacillus* spp, and *Desulfobacterium* spp.), Gammaproteobacteria, and Bacteroidetes. However no Firmicutes, including endospore-forming bacteria, were enriched in this group.

Discussion

The sampling sites in this study were selected with the objective to retrieve sediments differently impacted by the TMs released with the effluent from a WWTP. In the model system studied here, the WWTP of the City of Lausanne, previous studies suggested that the release of treated wastewater was correlated with high TM concentration in the sediments clustered around the outlet pipe (Thevenon et al. 2011a, b; Poté et al. 2008; Wildi et al. 2004; Pardos et al. 2004; Loizeau et al. 2004; Bravo et al.

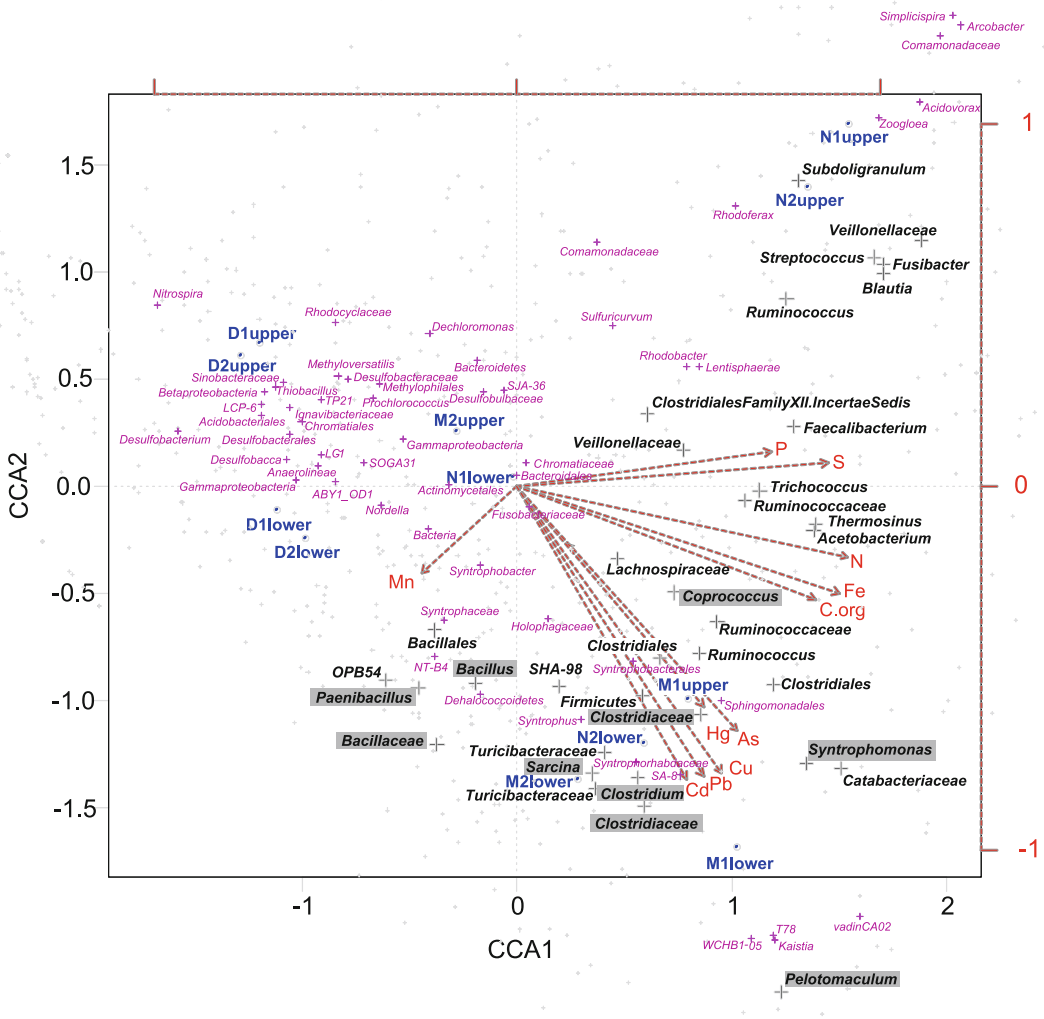

Fig. 4 Canonical correspondence analysis (CCA) triplot of the samples (*blue text* and *dots*) based on the bacterial groups identified in the sediment of the Vidy Bay and constrained by environmental variables. The ordination plot of the samples was constructed with results of OTUs picking and identification with the program QIIME from pyrosequencing data. Each OTU is represented by a cross in the plot. OTUs from sequences corresponding to less than 1 % (non Firmicutes) or 0.1 % (Firmicutes) of the community are shown in *light grey* crosses. OTUs representing non-Firmicutes are shown in *purple* and with *letters* in a *small font size*. OTUs corresponding to Firmicutes are shown in *black* and with a *larger font size*. Those assigned to endospore-forming Firmicutes are highlighted in *grey*. Additionally the centroids corresponding to the different environmental variables are represented by *dashed red arrows* (color figure online)

2011). However, this was not observed in the present study, in which contaminated sediments were also found relatively far from the outlet pipe. In addition, TM_{part} concentrations measured near the outlet pipe were much lower compared to those previously published (Poté et al. 2008), but similar to values published more recently (Haller et al. 2011), both reporting measurements from sediments collected in 2005, which corresponded to 16.8 cm deep according to a sedimentation rate of 2.8 cm/year (Loizeau et al. 2003). A reason for the differences observed could be that the deposition of organic matter and TM close to the outlet pipe is highly heterogeneous (Masson and Tercier-Waeber 2013). This is supported by the chemical characterization of cores N1 and N2, which were obtained from the area near the outlet pipe. For example, in core N1, a relatively low level of TM_{part} was detected for both layers. On the contrary, TM_{part} concentrations in the two layers of the core N2 were different, with low TM_{part} values for the upper layer and very high values for the lower layer. Probably the most surprising result was that the other samples with the highest TM_{part} levels (M1upper, M1lower and M2lower) were not retrieved near the outlet pipe, but rather in the intermediate area (Fig. 1b, c), which was supposedly less influenced by the direct release of treated wastewater. This could be directly linked to the transport of TM_{part} associated to

sediment particles or colloids with different size, which will influence sedimentation rate. However this cannot be evaluated based on the results since only bulk measurements were made. In addition, another element that needs to be considered in the future is the TM_{part} speciation linked to redox gradients or different mineral or organic fractions in the sediments. This is important since other studies have shown microzonation and redox gradients occurring at a millimeter scale can influence the availability of metals, as well as microbial communities or the biogeochemical processes affected by those (Huerta-Diaz et al. 2012).

A correlation was observed between $C_{org\text{-}part}$, $N_{org\text{-}part}$ and TM concentrations. In all the TM-contaminated sediments an increased $C_{org\text{-}part}$ and $N_{org\text{-}part}$ content was observed. This could be explained by an inhibitor effect of TM on microbial activity, as previously suggested for contaminated soils (Giller et al. 1998). Indeed, even low TM concentrations in soil have been shown to lead to the loss of functional diversity, reducing the diversity of metabolic pathways and impacting mineralization and nutrient cycling (Kandeler et al. 1996). Although a decrease in abundance and bacterial diversity (Table 2) was observed for samples with high levels of TM_{part}, the correlation with TMs was not significant (Supplementary Fig. 1). Alternatively the high concentration of $C_{org\text{-}part}$, $N_{org\text{-}part}$ and TM, as well as the absence of a correlation of the later with bacterial diversity can be the result of processes of transport and speciation associated with the deposition and accumulation of sediments derived from the treated wastewater, which is enriched in organic C, N, and TM, and that were not considered in this study, but have been analyzed elsewhere (Gascon Diez et al. 2013).

However, the release of treated wastewater clearly influenced bacterial abundance, which was highest in the upper layer of sediments retrieved near the outlet pipe, similarly to findings from a previous report (Thevenon et al. 2011b). Along with the WWTP effluent, not only large quantities of nutrients but also bacteria are directly released and probably deposited in the nearby sediments. This hypothesis is supported by the results of pyrosequencing revealing that *A. defluvii* and *H. caeni*, both typically found in activated sludge (Chung et al. 2007; Schulze et al. 1999), are the most abundant species in these samples.

A clear correlation was observed between endospore-forming bacteria and high levels of total particulate TMs (Fig. 4). Indeed, endospore-forming bacteria related to *Clostridium* spp., belonging to the Firmicutes, were detected in large proportions (representing close to 50 % of the total bacterial community) in samples with high TM_{part} contents. The species identified as the closest relatives to the sequences from the sediments corresponded to bacterial species previously linked to wastewater contamination. For example, *C. lituseburense*, which represents up to 21 % of the communities and was the most dominant OTU in TM contaminated sediments, was previously found in human feces (Franks et al. 1998) or abundant in wastewater effluents from dairy farms (McGarvey et al. 2004). Other two dominant species, *C. bartlettii* and *C. disporicum*, were also detected in human (Song et al. 2004; Mangin et al. 2004) or animal feces (Kobayashi et al. 2011; Horn 1987). Similar to *H. caeni* and *A. defluvii*, these three *Clostridium* species were probably released with the WWTP effluent, but contrary to the first two species, they seemed to be favored in the highly TM contaminated sediments. This was clearly demonstrated when comparing the cores N1 and N2. Although bacterial communities were very similar in the upper layer of both cores, as revealed by the DGGE analysis (Fig. 2) and the CCA (Fig. 4), they were completely different in the lower layer. For the low contaminated sample (N1lower) even though *C. lituseburense* was detected in small proportions, no bacteria seemed to dominate as indicated by a relatively high evenness (Table 2). In the sample with high TM_{part} levels (N2lower), *Clostridium* spp., and most particularly *C. lituseburense* (Supplementary Fig. 3), clearly prevailed and the functional diversity was arguably lower. The dominance of bacteria known for a fermentative metabolism could represent a reduction of OM degradation and a blockage of mineralization at the level of fermentation products, which could explain the accumulation of $C_{org\text{-}part}$ and $N_{org\text{-}part}$ observed here. The same interpretation is valid for the other highly TM contaminated sediments (M1upper, M1lower and M2lower).

Even though the dominant Clostridia species originate at the WWTP, it is still unclear if the correlation between high TM_{part} concentrations and dominance of these endospore-forming Firmicutes simply represent variations in the functioning of the WWTP. For example, one explanation could be that these bacteria are dominant in the microbial community at the WWTP during phases in which TM values are higher. However, the dominance of Firmicutes in wastewater treatment plants has not been reported in recent analyses of microbial communities by high throughput sequencing (Hu et al. 2012; Xia et al. 2010). This will favor a second hypothesis, better supported by the results, involving a selection mechanism driven by high load of TMs and leading to the dominance of Clostridia.

However an open question still remaining is why do TMs accumulate in certain areas. As filaments of *Beggiatoa sp.* were observed during the sampling campaign at the surface of sediments corresponding to the core M1 (containing high TM_{part} levels), and as this genus is known for sulfur-oxidation (Hagen and Nelson 1997), a role of sulfur in the adsorption of TM onto the solid sediment in these underlying layers was suspected. Sulfur was quantified in

order to assess the plausibility of this explanation. Even if a correlation was found between sediment total particulate iron and sulfur (Supplementary Fig. 1), possibly through the formation of pyrite (FeS_2) or mackinawite (FeS), no correlation was found between total particulate sulfur and TM, suggesting another mechanism for metal accumulation on the sediment.

In conclusion, sediments in the Vidy Bay were impacted by the WWTP effluent. The highest TM concentrations measured were 2 (Cu) to 18 (Hg) times higher than the probable effect levels (PELs) indicated by the Canadian Sediment Quality Guidelines (CCME 1999). These sediments are also significantly contaminated, accordingly to ICPR (2009) and therefore still represent a threat for aquatic organisms, as well as humans. The strong focus put on the methodology used to improve the recovery of DNA from sediments allowed a deeper characterization of the spatial distribution of the bacterial communities found in the surface sediments. In particular, while Proteobacteria and Bacteroidetes have been reported in the past as the dominant bacterial groups found in the Vidy Bay (Haller et al. 2011), a large proportion of endospore-forming Firmicutes (*Clostridium* spp.) was found in the present study. *C. lituseburense, C. bartlettii* and *C. disporicum* are all typically found in human feces, suggesting that they are probably released by the WWTP sewage effluent together with the TMs. This is supported by the strong correlation observed between endospore-forming bacteria and high TM_{part} concentrations (Fig. 4). However, the understanding of the underlying mechanisms explaining the relationship between endospore-forming bacteria and TM sorption on sediments requires further research. The fact that other bacterial groups associated to the WWTP effluent are not correlated with increased TM_{part} levels points out to a potentially active role of endospores in TM transport and deposition on sediments. Therefore endospore-forming bacteria can be a missing biological link to understand the role of sediment as sink or source of TM contamination. However, other alternatives including factors such as the spatiotemporal variation of the microbiological and chemical composition of the treated effluent, or processes controlling microbial communities such as predation, need to be explored in the future.

Acknowledgments This publication is part of the international, interdisciplinary research project ELEMO (http://www.elemo.ch) to investigate the deep-waters of Lake Geneva using two Russian MIR submarines. Funding for this study was provided by the Fondation pour l'Etude des Eaux du Léman (FEEL). Additional funding for the work described in this paper was provided by the Swiss National Science Foundation (Grant 31003A_132358). We are grateful for the support. We thank the Russian MIR crew members (http://www.elemo.ch/mir-team) for their excellent performance and the SAGRAVE team who provided and operated the platform from which the dives were carried out. We also thank Ulrich Lemmin and Jean-Denis Bourquin for project coordination. The service of Mikhail Kranoperov (Russian Honorary Consulate) as liaison is greatly appreciated. Special thanks to Jean-Claude Lavanchy from the Centre of Mineral Analysis (CAM), University of Lausanne, for helping with elemental analysis, and Radu Slobodeanu, from the University of Neuchâtel, for helping on statistical analysis. The authors thank two anonymous reviewers for the valuable comments to improve this manuscript.

References

Altschul SF, Gish W, Miller W, Myers EW, Lipman DJ (1990) Basic local alignment search tool. J Mol Biol 215(3):403–410

Anderson RT, Vrionis HA, Ortiz-Bernad I, Resch CT, Long PE, Dayvault R, Karp K, Marutzky S, Metzler DR, Peacock A, White DC, Lowe M, Lovley DR (2003) Stimulating the in situ activity of *Geobacter* species to remove uranium from the groundwater of a uranium-contaminated aquifer. Appl Environ Microbiol 69(10):5884–5891

Bakke I, De Schryver P, Boon N, Vadstein O (2011) PCR-based community structure studies of Bacteria associated with eukaryotic organisms: a simple PCR strategy to avoid co-amplification of eukaryotic DNA. J Microbiol Methods 84(2):349–351

Batten KM, Scow KM (2003) Sediment microbial community composition and methylmercury pollution at four mercury mine-impacted sites. Microb Ecol 46(4):429–441

Benoit JM, Gilmour CC, Heyes A, Mason RP, Miller CL (2003) Geochemical and biological controls over methylmercury production and degradation in aquatic ecosystems. Biogeochem Environ Important Trace Elem 835:262–297

Berg J, Brandt KK, Al-Soud WA, Holm PE, Hansen LH, Sørensen SJ, Nybroe O (2012) Selection for Cu-tolerant bacterial communities with altered composition, but unaltered richness, via long-term Cu exposure. Appl Environ Microbiol 78(20):7438–7446

Blanck H (2002) A critical review of procedures and approaches used for assessing pollution-induced community tolerance (PICT) in biotic communities. Hum Ecol Risk Assess 8(5):1003–1034

Blanck H, Wangberg SA, Molander S (1988) Pollution-induced community tolerance—a new ecotoxicological tool. In: Cairns J, Pratt JR (eds) Functional testing of aquatic biota for estimating hazards of chemicals, ASTM STP 988. American Society for Testing and Materials, Philadelphia, pp 219–230

Bravo AG, Bouchet S, Amouroux D, Pote J, Dominik J (2011) Distribution of mercury and organic matter in particle-size classes in sediments contaminated by a waste water treatment plant: Vidy Bay, Lake Geneva, Switzerland. J Environ Monit 13(4):974–982

Caporaso JG, Kuczynski J, Stombaugh J, Bittinger K, Bushman FD, Costello EK, Fierer N, Pena AG, Goodrich JK, Gordon JI, Huttley GA, Kelley ST, Knights D, Koenig JE, Ley RE, Lozupone CA, McDonald D, Muegge BD, Pirrung M, Reeder J, Sevinsky JR, Tumbaugh PJ, Walters WA, Widmann J, Yatsunenko T, Zaneveld J, Knight R (2010) QIIME allows analysis of high-throughput community sequencing data. Nat Methods 7(5):335–336

CCME (1999) Canadian sediment quality guidelines for the protection of aquatic life. Reprinted in Canadian environmental quality guidelines, Chapter 6. Canadian Council of Ministers of the Environment, Winnipeg.

Chang YJ, Peacock AD, Long PE, Stephen JR, McKinley JP, Macnaughton SJ, Hussain AK, Saxton AM, White DC (2001) Diversity and characterization of sulfate-reducing bacteria in groundwater at a uranium mill tailings site. Appl Environ Microbiol 67(7):3149–3160

Chung BS, Ryu SH, Park M, Jeon Y, Chung YR, Jeon CO (2007) *Hydrogenophaga caeni* sp. nov., isolated from activated sludge. Int J Syst Evol Microbiol 57:1126–1130

Colwell RK, Coddington JA (1994) Estimating terrestrial biodiversity through extrapolation. Philos Trans R Soc Lond B Biol Sci 345(1311):101–118

Daims H, Lucker S, Wagner M (2006) daime, a novel image analysis program for microbial ecology and biofilm research. Environ Microbiol 8(2):200–213

Dineen SM, Aranda R, Anders DL, Robertson JM (2010) An evaluation of commercial DNA extraction kits for the isolation of bacterial spore DNA from soil. J Appl Microbiol 109(6):1886–1896

Dorioz JM, Pelletier JP, Benoit P (1998) Physico-chemical properties and bioavailability of particulate phosphorus of various origin in a watershed of Lake Geneva (France). Water Res 32(2):275–286

Errington J (2003) Regulation of endospore formation in *Bacillus subtilis*. Nat Rev Microbiol 1(2):117–126

Ferris MJ, Muyzer G, Ward DM (1996) Denaturing gradient gel electrophoresis profiles of 16S rRNA-defined populations inhabiting a hot spring microbial mat community. Appl Environ Microbiol 62(2):340–346

Förstner U, Wittmann GTW (1981) Metal pollution in the aquatic environment, 2nd rev. edn. Springer-Verlag, New York, Heidelberg, Berlin

Franks AH, Harmsen HJM, Raangs GC, Jansen GJ, Schut F, Welling GW (1998) Variations of bacterial populations in human feces measured by fluorescent in situ hybridization with group-specific 16S rRNA-targeted oligonucleotide probes. Appl Environ Microbiol 64(9):3336–3345

Gascon Diez E, Bravo AG, a Porta N, Masson M, Graham ND, Stoll S, Akhtman Y, Amouroux D, Loizeau JL (2013) Mercury content and speciation related to sediment surface patterns in contaminated Vidy Bay, Lake Geneva, Switzerland. Aquat Sci (this issue)

Giller KE, Witter E, McGrath SP (1998) Toxicity of heavy metals to microorganisms and microbial processes in agricultural soils: a review. Soil Biol Biochem 30(10–11):1389–1414

Gough HL, Stahl DA (2011) Microbial community structures in anoxic freshwater lake sediment along a metal contamination gradient. ISME J 5(3):543–558

Hagen KD, Nelson DC (1997) Use of reduced sulfur compounds by *Beggiatoa* spp.: enzymology and physiology of marine and freshwater strains in homogeneous and gradient cultures. Appl Environ Microbiol 63(10):3957–3964

Haller L, Tonolla M, Zopfi J, Peduzzi R, Wildi W, Pote J (2011) Composition of bacterial and archaeal communities in freshwater sediments with different contamination levels (Lake Geneva, Switzerland). Water Res 45(3):1213–1228

Harris D, Horwath WR, van Kessel C (2001) Acid fumigation of soils to remove carbonates prior to total organic carbon or carbon-13 isotopic analysis. Soil Sci Soc Am J 65(6):1853–1856

Hines ME, Horvat M, Faganeli J, Bonzongo JC, Barkay T, Major EB, Scott KJ, Bailey EA, Warwick JJ, Lyons WB (2000) Mercury biogeochemistry in the Idrija river, Slovenia, from above the mine into the Gulf of Trieste. Environ Res 83(2):129–139

Horn N (1987) *Clostridium disporicum* sp-nov, a saccharolytic species able to form 2 spores per cell, isolated from a rat cecum. Int J Syst Bacteriol 37(4):398–401

Hu M, Wang X, Wen X, Xia Y (2012) Microbial community structures in different wastewater treatment plants as revealed by 454-pyrosequencing analysis. Bioresour Technol 117:72–79

Huerta-Diaz MA, Delgadillo-Hinojosa F, Siqueiros-Valencia A, Valdivieso-Ojeda J, Reimer JJ, Segovia-Zavala JA (2012) Millimeter-scale resolution of trace metal distributions in microbial mats from a hypersaline environment in Baja California, Mexico. Geobiology 10(6):531–547

ICPR (2009) Sediment management plan Rhine: summary. Report No. 175, International Commission for the Protection of the Rhine (ICPR), Koblenz

Kandeler E, Kampichler C, Horak O (1996) Influence of heavy metals on the functional diversity of soil microbial communities. Biol Fertil Soils 23(3):299–306

Kerin EJ, Gilmour CC, Roden E, Suzuki MT, Coates JD, Mason RP (2006) Mercury methylation by dissimilatory iron-reducing bacteria. Appl Environ Microbiol 72(12):7919–7921

Kobayashi Y, Itoh A, Miyawaki K, Koike S, Iwabuchi O, Iimura Y, Kobashi Y, Kawashima T, Wakamatsu J, Hattori A, Murakami H, Morimatsu F, Nakaebisu T, Hishinuma T (2011) Effect of liquid whey feeding on fecal microbiota of mature and growing pigs. Anim Sci J 82(4):607–615

Li H, Zhang Y, Li DS, Xu H, Chen GX, Zhang CG (2009) Comparisons of different hypervariable regions of rrs genes for fingerprinting of microbial communities in paddy soils. Soil Biol Biochem 41(5):954–968

Loizeau J-L, Rozé S, Peytremann C, Monna F, Dominik J (2003) Mapping sediment accumulation rate by using volume magnetic susceptibility core correlation in a contaminated bay (Lake Geneva, Switzerland). Eclogae Geol Helv 96(Supplement 1):S73–S79

Loizeau J-L, Pardos M, Monna F, Peytremann C, Haller L, Dominik J (2004) The impact of a sewage treatment plant's effluent on sediment quality in a small bay in Lake Geneva (Switzerland–France). Part 2: temporal evolution of heavy metals. Lakes Reserv: Res Manag 9:53–63

Mangin I, Bonnet R, Seksik P, Rigottier-Gois L, Sutren M, Bouhnik Y, Neut C, Collins MD, Colombel JF, Marteau P, Dore J (2004) Molecular inventory of faecal microflora in patients with Crohn's disease. FEMS Microbiol Ecol 50(1):25–36

Masson M, Tercier-Waeber ML (2013) Trace metal speciation at the sediment-water interface of the Vidy Bay: influence of contrasting sediment characteristics. Aquat Sci (this issue)

McGarvey JA, Miller WG, Sanchez S, Stanker L (2004) Identification of bacterial populations in dairy wastewaters by use of 16S rRNA gene sequences and other genetic markers. Appl Environ Microbiol 70(7):4267–4275

Murphy J, Riley JP (1962) A modified single solution method for determination of phosphate in natural waters. Anal Chim Acta 27(1):31–36

Muyzer G, Dewaal EC, Uitterlinden AG (1993) Profiling of complex microbial populations by denaturing gradient gel electrophoresis analysis of polymerase chain reaction-amplified genes coding for 16 s rRNA. Appl Environ Microbiol 59(3):695–700

Nakagawa T, Hanada S, Maruyama A, Marumo K, Urabe T, Fukui M (2002) Distribution and diversity of thermophilic sulfate-reducing bacteria within a Cu-Pb-Zn mine (Toyoha, Japan). FEMS Microbiol Ecol 41(3):199–209

Nealson KH (1997) Sediment bacteria: who's there, what are they doing, and what's new? Annu Rev Earth Planet Sci 25:403–434

Nevin KP, Holmes DE, Woodard TL, Hinlein ES, Ostendorf DW, Lovley DR (2005) *Geobacter bemidjiensis* sp nov and *Geobacter psychrophilus* sp nov., two novel Fe(III)-reducing subsurface isolates. Int J Syst Evol Microbiol 55:1667–1674

Ogilvie LA, Grant A (2008) Linking pollution induced community tolerance (PICT) and microbial community structure in chronically metal polluted estuarine sediments. Mar Environ Res 65(2):187–198

Pardos M, Benninghoff C, Alencastro LP, Wildi W (2004) The impact of a sewage treatment plant's effluent on sediment quality in a small bay in Lake Geneva (Switzerland–France). Part 1:

spatial distribution of contaminants and the potential for biological impacts. Lakes Reserv: Res Manage 9:41–52

Poté J, Haller L, Loizeau J-L, Garcia Bravo A, Sastre V, Wildi W (2008) Effects of a sewage treatment plant outlet pipe extension on the distribution of contaminants in the sediments of the Bay of Vidy, Lake Geneva, Switzerland. Bioresour Technol 99(15):7122–7131

Ramette A (2007) Multivariate analyses in microbial ecology. FEMS Microbiol Ecol 62(2):142–160

Sánchez-Andrea I, Knittel K, Amann R, Amils R, Sanz JL (2012) Quantification of Tinto river sediment microbial communities: importance of sulfate-reducing bacteria and their role in attenuating acid mine drainage. Appl Environ Microbiol 78(13):4638–4645

Schloss PD, Handelsman J (2005) Introducing DOTUR, a computer program for defining operational taxonomic units and estimating species richness. Appl Environ Microbiol 71(3):1501–1506

Schulze R, Spring S, Amann R, Huber I, Ludwig W, Schleifer KH, Kampfer P (1999) Genotypic diversity of *Acidovorax* strains isolated from activated sludge and description of *Acidovorax defluvii* sp nov. Syst Appl Microbiol 22(2):205–214

Schwarzenbach RP, Escher BI, Fenner K, Hofstetter TB, Johnson CA, von Gunten U, Wehrli B (2006) The challenge of micropollutants in aquatic systems. Science 313(5790):1072–1077

Selin NE (2009) Global biogeochemical cycling of mercury: a review. Annu Rev Environ Resour 34:43–63

SESA (2012) Bilans 2011 de l'épuration vaudoise. Service des eaux, sols et assainissement

Shipp WG, Zierenberg RA (2008) Pathways of acid mine drainage to Clear Lake: implications for mercury cycling. Ecol Appl 18(8 Suppl):A29–A54

Song YL, Liu CX, McTeague M, Summanen P, Finegold SM (2004) *Clostridium bartlettii* sp nov., isolated from human faeces. Anaerobe 10(3):179–184

Stackebrandt E, Goebel BM (1994) Taxonomic note: a place for DNA–DNA reassociation and 16S rRNA sequence analysis in the present species definition in bacteriology. Int J Syst Evol Microbiol 44(4):846–849

Tercier-Waeber M-L, Stoll S, Slaveykova VI (2012) Trace metal behavior in surface waters: emphasis on dynamic speciation, sorption processes and bioavailability. Arch Sci 65:119–142

Thevenon F, Graham ND, Chiaradia M, Arpagaus P, Wildi W, Pote J (2011a) Local to regional scale industrial heavy metal pollution recorded in sediments of large freshwater lakes in central Europe (lakes Geneva and Lucerne) over the last centuries. Sci Total Environ 412:239–247

Thevenon F, Graham ND, Herbez A, Wildi W, Pote J (2011b) Spatio-temporal distribution of organic and inorganic pollutants from Lake Geneva (Switzerland) reveals strong interacting effects of sewage treatment plant and eutrophication on microbial abundance. Chemosphere 84(5):609–617

Weinbauer MG, Beckmann C, Hofle MG (1998) Utility of green fluorescent nucleic acid dyes and aluminum oxide membrane filters for rapid epifluorescence enumeration of soil and sediment bacteria. Appl Environ Microbiol 64(12):5000–5003

Wildi W, Dominik J, Loizeau JL, Thomas RL, Favarger P-Y, Haller L, Perroud A, Peytremann C (2004) River, reservoir and lake sediment contamination by heavy metals downstream from urban areas of Switzerland. Lakes Reserv: Res Manag 9:75–87

Xia S, Duan L, Song Y, Li J, Piceno YM, Andersen GL, Alvarez-Cohen L, Moreno-Andrade I, Huang CL, Hermanowicz SW (2010) Bacterial community structure in geographically distributed biological wastewater treatment reactors. Environ Sci Technol 44(19):7391–7396

Yu R-Q, Flanders JR, Mack EE, Turner R, Mirza MB, Barkay T (2012) Contribution of coexisting sulfate and iron reducing bacteria to methylmercury production in freshwater river sediments. Environ Sci Technol 46(5):2684–2691

Zhang YJ, Bryan ND, Livens FR, Jones MN (1996) Complexing of metal ions by humic substances. Humic Fulvic Acids: Isol Struct Environ Role 651:194–206